of 0.41 in the full basis or 0.34 in the no4s4p basis is the largest of any of the 3d orbitals. If one assumes that all the bonding orbital occupations contribute to metal–ligand bonding, the V–V bond order would be between 1.59 and 1.86. Thus our minimum estimate of the V–V bond order comes from the difference between bonding and anti-bonding populations and is 0.58, while our upper estimate, based only on the bonding populations, is 1.86 V–V bonds. Thus the calculations support the interpretation of the experiment that direct V–V bonding exists but suggest that it is not as strong as a V–V double bond with some triple bond character.

Since the experiments show the presence of a low-lying triplet state, we have also considered two triplet states arising from single excitations into the $30a_1$ V–V bonding orbital, by using only the no4s4p basis set. The $^3B_1$ state arising from the single excitation $26b_1 \rightarrow 30a_1$ is considerably lower than the $^3A_2$ state arising from $14a_2 \rightarrow 30a_1$. The $^3B_1$ state arises from moving a V–V anti-bonding electron into a V–V bonding orbital, while the $^3A_2$ state arises from moving a ligand electron into a V–V bonding orbital. As in the case of the closed-shell occupations, exciting from the ligand orbital is less favorable. The $26b_1^1 \rightarrow 30a_1^1$ excitation leads to a state lower in energy than the lowest closed-shell occupation (3). SCF wave functions do not describe closed-shell singlet and triplet states equally well. This is a result of the singlet state having one more doubly occupied orbital than the triplet. A rule of thumb is that each electron pair has about one eV more correlation energy than a pair of high spin coupled-open shell electrons. Therefore, the one extra bonding pair of electrons in the singlet state will lead to about one eV more correlation in the singlet state. Thus with the inclusion of correlation, it is expected that the $^1A_1$ and $^3B_1$ states would be very close in energy. By comparing these calculations with experiment[1,3] it is highly likely that the $^1A_1$ state from occupation (3) is the ground state and the $^3B_1$ state is the triplet state that causes a change in the magnetic properties with increased temperature. The $26b_1^1 \rightarrow 30a_1^1$ excitation moves an electron from an orbital which is metal–metal anti-bonding and metal–ligand bonding, into an orbital which is metal–metal bonding. This suggests a similar magnitude for the energetics for the two bonding mechanisms. Thus, the presence of a low-lying triplet state does not suggest that the V–V bonding is weak and that a V–V bond is breaking. In fact the V–V bonding character is probably increasing, (compare the bond orders for the two states in Table III) and the bonding in this system is rather a complex balance between V–V and vanadium–ligand bonding.

IV. Conclusions

The calculations show that there is a direct V–V 3d bond. However, the interaction is complex because of the 3d involvement in both the metal–metal and metal–ligand bonding. Therefore, 3d orbitals which are V–V anti-bonding can be occupied if at the same time they are vanadium ligand bonding. This leads to the lowest closed-shell occupation, while the occupation which arises by only considering V–V 3d interactions is 3.6 eV higher. The low-lying triplet state does not arise by breaking a weak metal–metal bond but rather by promoting an electron from a metal–ligand bonding orbital into a metal–metal orbital.

Reactions of Carbon Monoxide with Trimethylsilyl and Tris(trimethylsilyl)silyl Derivatives of Group 4 Metals. Synthesis, Characterization, and Reactivity of Silaacyl Complexes

Brian K. Campion, Jonathan Falk, and T. Don Tilley*

Contribution from the Chemistry Department, D-006, University of California at San Diego, La Jolla, California 92093. *Received September 15, 1986*

Abstract: The new silyl derivatives $Cp_2M[Si(SiMe_3)_3]Cl$ ($Cp = \eta^5\text{-}C_5H_5$; **3**, M = Zr; **4**, M = Hf), $Cp_2ClZr(\mu\text{-}O)ZrCp_2[Si(SiMe_3)_3]$ (**5**), and $Cp_2Zr[Si(SiMe_3)_3]SiMe_3$ (**6**) are prepared by reaction of $(THF)_3LiSi(SiMe_3)_3$ with the appropriate metal halide. The compounds $Cp_2Zr[Si(SiMe_3)_3]BH_4$ (**7**) and $Cp_2Zr[Si(SiMe_3)_3]Me$ (**8**) are obtained from reaction of **3** with $LiBH_4$ and MeMgBr, respectively. Reaction of $Cp_2Zr(SiMe_3)Cl$ (**1**) with carbon monoxide provides the silaacyl $Cp_2Zr(\eta^2\text{-}COSiMe_3)Cl$ (**9**) and the first observation of carbon monoxide insertion into a transition-metal–silicon bond. Complex **9** is isolated in 90% yield and has been characterized by its spectral properties and crystal structure, which establishes bidentate ligation of the silaacyl group. Crystals of **9** belong to space group $P2_1/n$, with $a = 9.7608$ (12) Å, $b = 12.8694$ (16) Å, $c = 12.6837$ (15) Å, $\beta = 91.074$ (10)°, $V = 1593.0$ (6) Å^3, and $Z = 4$. In contrast, carbonylation of **3** does not yield an isolable silaacyl complex. Carbonylation of **6** and **8** produce the acyl derivatives $Cp_2Zr(\eta^2\text{-}COSiMe_3)[Si(SiMe_3)_3]$ (**11**) and $Cp_2Zr(\eta^2\text{-}COMe)[Si(SiMe_3)_3]$ (**12**), respectively. The titanium silyl $Cp_2Ti(SiMe_3)Cl$ reacts cleanly with carbon monoxide by an apparent ligand-induced reductive elimination to produce $Cp_2Ti(CO)_2$ and Me_3SiCl. Compound **9** does not react with pyridine but with $2,6\text{-}Me_2C_6H_3NC$; the ketenimine complex $Cp_2Zr[OC(SiMe_3)(CN\text{-}2,6\text{-}Me_2C_6H_3)]Cl$ (**14**), characterized in solution, is formed. Complex **9** reacts with $LiOCMe_3$ via decarbonylation to give $Cp_2Zr(SiMe_3)(OCMe_3)$. Electrophiles $Me_3SiOSO_2CF_3$ or $MeOSO_2CF_3$ react with **9** to afford $Cp_2Zr(\eta^2\text{-}COSiMe_3)(OSO_2CF_3)$ and Me_3SiCl or MeCl, respectively. Protonation of **11** with benzoic acid produces the benzoate complex $Cp_2Zr[Si(SiMe_3)_3](\eta^2\text{-}O_2CPh)$ (**16**). Insertion of the isocyanide $2,6\text{-}Me_2C_6H_3NC$ into the Zr–Si bonds of **1** and **3** occurs readily to give $Cp_2Zr[\eta^2\text{-}C(N\text{-}2,6\text{-}Me_2C_6H_3)SiMe_3]Cl$ (**17**) and $Cp_2Zr[\eta^2\text{-}C(N\text{-}2,6\text{-}Me_2C_6H_3)Si(SiMe_3)_3]Cl$ (**18**), respectively. The Zr–Si bond of **1** is cleaved rapidly by H_2 to give $[Cp_2ZrHCl]_n$ and $HSiMe_3$. Compound **6** reacts similarly with H_2 to afford $HSiMe_3$ and $HSi(SiMe_3)_3$ quantitatively. No reactions were observed between **1** and ethylene, phenylacetylene, benzonitrile, carbon dioxide, or carbon disulfide nor between **3** and phenylacetylene, 4-methoxybenzonitrile, or phenyl isocyanate.

Numerous unsaturated molecules are catalytically or stoichiometrically reduced by transition-metal–silane systems.[1-4] The degree to which insertions into M–Si bonds contribute to this reactivity is unclear, since few insertions involving metal–silicon

0002-7863/87/1509-2049$01.50/0 © 1987 American Chemical Society

bonds have been directly observed.[4,5] Insertion of carbon monoxide has long been considered unfavorable, since attempts to carbonylate metal silyl derivatives have previously failed.[5,6] This low reactivity toward insertions is consistent with observations that transition-metal–silicon bonds are shorter than expected, presumably strengthened by π-bonding between the transition metal and silicon.[5]

The only previously reported silaacyl complex, *fac*-$Re(CO)_3(dppe)(COSiPh_3)$ (dppe = $Ph_2PCH_2CH_2PPh_2$), decarbonylates irreversibly above 182 °C. This compound, prepared by addition of Ph_3SiLi to $[Re(CO)_4(dppe)]ClO_4$, could not be obtained by subjecting the decarbonylation product, *mer*-$Re(CO)_3(dppe)(SiPh_3)$, to a CO pressure of 300 atm.[7] Migratory insertion reactions of some kind may occur in decompositions of a few silyl–carbonyl complexes. These reactions all lead to siloxide derivatives by ill-defined processes that involve inter- or intramolecular silyl migration,[5,8] and most commonly result in cleavage of the carbon monoxide C–O bond (e.g., eq 1[8a]). A similar

$$H_3SiV(CO)_6 \xrightarrow{25\ °C} H_3SiOSiH_3 + V(CO)_6 + [V(CO)_5C] \tag{1}$$

deoxygenation of CO has been carried out in the nickel-catalyzed synthesis of siloxanes from hexamethyldisilane.[9] Sufficiently reactive transition-metal–silyl complexes therefore have the potential to activate CO in unique ways. Furthermore, such processes might provide new routes to acylsilanes, which are important intermediates in organic synthesis.[10]

Our studies concerned with early transition-metal–silyl reactivity[11] have included reactions with carbon monoxide in order to elucidate the factors involved in silyl migration to coordinated CO. The tendency of M–Si bonds in d^0 complexes to insert unsaturated substrates was expected to be greater than in previously studied complexes, since bond strengthening by metal-to-silicon π-donation cannot occur. Crystal structures of two zirconium silyl compounds[11a,12] indeed reveal rather long Zr–Si bonds. We report herein the preparation of zirconium and hafnium derivatives of $-Si(SiMe_3)_3$ and the reactions of these and other early transition-metal silyls with CO. These results include the first observation of CO insertion into a transition-metal–silicon bond and the X-ray crystal structure of the silaacyl complex $Cp_2Zr(\eta^2\text{-}COSiMe_3)Cl$ (**9**, Cp = $\eta^5\text{-}C_5H_5$). Part of this work has been communicated.[11b]

Results and Discussion

Preparation of New Silyl Complexes. The silyllithium $(THF)_3LiSi(SiMe_3)_3$[13] is a useful reagent for preparing a number of zirconium and hafnium silyl species. Tris(trimethylsilyl)silyl derivatives analogous to the previously reported $Cp_2M(SiMe_3)Cl$ (**1**, M = Zr; **2**, M = Hf)[11a] are obtained on reaction of the metallocene dichlorides with $(THF)_3LiSi(SiMe_3)_3$ (eq 2).

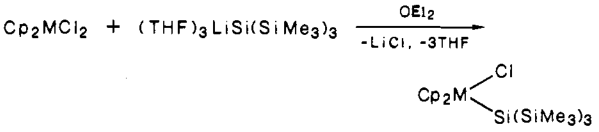

$$Cp_2MCl_2 + (THF)_3LiSi(SiMe_3)_3 \xrightarrow[-LiCl,\ -3THF]{OEt_2} Cp_2M(Cl)Si(SiMe_3)_3 \tag{2}$$

3, M = Zr
4, M = Hf

Pentane-soluble **3** and **4** are orange and yellow, respectively. Only one chlorine of $(Cp_2ZrCl)_2(\mu\text{-}O)$ is displaced on reaction with a twofold excess of $(THF)_3LiSi(SiMe_3)_3$ to produce the yellow dinuclear complex **5** (eq 3). Reaction of $(THF)_3LiSi(SiMe_3)_3$ with **1** affords the bis(silyl) complex **6** (eq 4), which crystallizes from pentane as intensely colored red prisms.

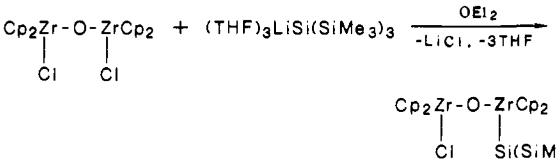

$$Cp_2Zr(Cl){-}O{-}ZrCp_2(Cl) + (THF)_3LiSi(SiMe_3)_3 \xrightarrow[-LiCl,\ -3THF]{OEt_2} Cp_2Zr(Cl){-}O{-}ZrCp_2(Si(SiMe_3)_3) \tag{3}$$

5

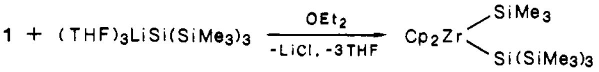

$$\mathbf{1} + (THF)_3LiSi(SiMe_3)_3 \xrightarrow[-LiCl,\ -3THF]{OEt_2} Cp_2Zr(SiMe_3)Si(SiMe_3)_3 \tag{4}$$

6

Other new silyl complexes are obtained by substitution of the chloride ligand in **3**. Yellow $Cp_2Zr[Si(SiMe_3)_3]BH_4$ (**7**), prepared from **3** and $LiBH_4$, has been shown by infrared spectroscopy to contain a bidentate borohydride ligand.[14] The yellow-orange alkyl–silyl complex $Cp_2Zr[Si(SiMe_3)_3]Me$ (**8**) was prepared similarly from **3** and MeMgBr. Spectroscopic data for all new compounds are given in Table I.

Reactions with Carbon Monoxide. Red diethyl ether or pentane solutions of **1** react with carbon monoxide with precipitation of a pink powder. This pink compound is insoluble in most hydrocarbons but can be crystallized from dichloromethane/diethyl ether mixtures. Spectroscopic data are consistent with CO insertion to produce the silaacyl complex $Cp_2Zr(\eta^2\text{-}COSiMe_3)Cl$ (**9**). The structure was confirmed by X-ray crystallography (vide infra). The carbonyl stretching frequency of this compound (1489 cm^{-1}) is similar to that of *fac*-$Re(CO)_3(diphos)(COSiPh_3)$ (ν_{CO} = 1490 cm^{-1}),[7] though the latter contains a monodentate silaacyl ligand. This value is considerably lower than those found in analogous zirconium acyls (1500–1550 cm^{-1}),[15] a fact that is consistent with

---

(1) (a) Speier, J. L. *Adv. Organomet. Chem.* **1978**, *17*, 407. (b) Cundy, C. S.; Kingston, B. M.; Lappert, M. F. *Adv. Organomet. Chem.* **1973**, *11*, 253.

(2) (a) James, B. R. *Adv. Organomet. Chem.* **1978**, *17*, 319. (b) Ojima, I.; Nihonyanagi, M.; Kogure, T.; Kumagai, M.; Horiuchi, S.; Nakatsugawa, K.; Nagai, Y. *J. Organomet. Chem.* **1975**, *94*, 449. (c) Ojima, I.; Kogure, T.; Kumagai, M. *J. Org. Chem.* **1977**, *42*, 1671. (d) Ojima, I.; Kogure, T. *Organometallics* **1982**, *1*, 1390. (e) Brunner, H.; Becker, R.; Riepl, G. *Organometallics* **1982**, *3*, 1354.

(3) (a) Murai, S.; Sonoda, N. *Angew. Chem., Int. Ed. Engl.* **1979**, *18*, 837. (b) Chatani, N.; Murai, S.; Sonoda, N. *J. Am. Chem. Soc.* **1983**, *105*, 1370. (c) Koinuma, H.; Kawakami, F.; Kato, H.; Hirai, H. *J. Chem. Soc., Chem. Commun.* **1981**, 213. (d) Kaplan, L. *Organometallics* **1982**, *1*, 1102.

(4) Gladysz, J. A. *Acc. Chem. Res.* **1984**, *17*, 326.

(5) (a) Aylett, B. J. *Adv. Inorg. Chem. Radiochem.* **1982**, *25*, 1. (b) Höfler, F. In *Topics in Current Chemistry*; Springer-Verlag: New York, Vol. 50, pp 129–165. (c) Ang, H. C.; Lau, P. T. *Organomet. Chem. Rev. A* **1972**, *8*, 235.

(6) (a) Redwood, M. E.; Reichert, B. E.; Schrieke, R. R.; West, B. O. *Aust. J. Chem.* **1973**, *26*, 247. (b) Hagan, A. P.; McAmis, L.; Stewart, M. A. *J. Organomet. Chem.* **1974**, *66*, 127. (c) Aylett, B. J.; Campbell, J. M. *J. Chem. Soc. A* **1969**, 1910. (d) de Charentenay, F.; Osborn, J. A.; Wilkinson, G. *J. Chem. Soc. A* **1968**, 787. (e) Aylett, B. J.; Campbell, J. M. *J. Chem. Soc., Chem. Commun.* **1967**, 159. (f) Hoyano, J. K.; Graham, W. A. G. *Inorg. Chem.* **1972**, *11*, 1265.

(7) Anglin, J. R.; Calhoun, H. P.; Graham, W. A. G. *Inorg. Chem.* **1977**, *16*, 2281.

(8) (a) Allinson, J. S.; Aylett, B. J.; Colquhoun, H. M. *J. Organomet. Chem.* **1976**, *112*, C7. (b) Schrieke, R. R.; West, B. O. *Aust. J. Chem.* **1969**, *22*, 49. (c) Ingle, W. M.; Petri, G.; MacDiarmid, A. G. *J. Chem. Soc., Chem. Commun.* **1973**, 497.

(9) Vollhardt, K. P. C.; Yang, Z.-Y. *Angew. Chem., Int. Ed. Engl.* **1984**, *23*, 460.

(10) (a) Seyferth, D.; Weinstein, R. M. *J. Am. Chem. Soc.* **1982**, *104*, 5534. (b) Reich, H. J.; Kelly, M. J. *J. Am. Chem. Soc.* **1982**, *104*, 119. (c) Brook, A. G. *Adv. Organomet. Chem.* **1968**, *7*, 95 and references cited in the above.

(11) (a) Tilley, T. D. *Organometallics* **1985**, *4*, 1452. (b) Tilley, T. D. *J. Am. Chem. Soc.* **1985**, *107*, 4084. (c) Arnold, J.; Tilley, T. D. *J. Am. Chem. Soc.* **1985**, *107*, 6409. (d) Arnold, J.; Shina, D. N.; Tilley, T. D.; Arif, A. M. *Organometallics* **1986**, *5*, 2037. (e) Arnold, J.; Tilley, T. D.; Rheingold, A. L. *J. Am. Chem. Soc.* **1985**, *108*, 5355. (f) Roddick, D. M.; Tilley, T. D., manuscript in preparation. (g) Elsner, F.; Tilley, T. D., manuscript in preparation.

(12) Muir, K. W. *J. Chem. Soc. A* **1971**, 2663.

(13) Gutekunst, G.; Brook, A. G. *J. Organomet. Chem.* **1982**, *225*, 1.

(14) Marks, T. J.; Kolb, J. R. *Chem. Rev.* **1977**, *77*, 263.

(15) (a) Marsella, J. A.; Huffman, J. C.; Caulton, K. G.; Longato, B.; Norton, J. R. *J. Am. Chem. Soc.* **1982**, *104*, 6360. (b) Marsella, J. A.; Moloy, K. G.; Caulton, K. G. *J. Organomet. Chem.* **1980**, *201*, 389. (c) Manriquez, J. M.; McAlister, D. R.; Sanner, R. D.; Bercaw, J. E. *J. Am. Chem. Soc.* **1978**, *100*, 2716. (d) Fachinetti, G.; Floriani, C.; Marchetti, F.; Merlino, S. *J. Chem. Soc., Chem. Commun.* **1976**, 522. (e) Bertelo, C. A.; Schwartz, J. *J. Am. Chem. Soc.* **1975**, *97*, 228. (f) Carr, D. B.; Schwartz, J. *J. Am. Chem. Soc.* **1979**, *101*, 3521. (g) Fachinetti, G.; Fochi, G.; Floriani, C. *J. Chem. Soc., Dalton Trans.* **1977**, 1946. (h) Erker, G.; Rosenfeldt, F. *Angew. Chem., Int. Ed. Engl.* **1978**, *17*, 605. (i) Jeffrey, J.; Lappert, M. F.; Luong-Thi, N. T.; Webb, M.; Atwood, J. L.; Hunter, W. E. *J. Chem. Soc., Dalton Trans.* **1981**, 1593. (j) Lappert, M. F.; Luong-Thi, N. T.; Milne, C. R. C. *J. Organomet. Chem.* **1979**, *174*, C35.

silyl substitution.[7,16] The ^1H NMR spectrum (dichloromethane-d_2) of $Cp_2Zr(\eta^2\text{-}^{13}COSiMe_3)Cl$ exhibits a singlet at 5.78 for the Cp ligands and a doublet at 0.47 ppm ($^3J_{CH}$ = 1.8 Hz) for the $-SiMe_3$ group. A similar coupling constant (2.4 Hz) was observed in $Cp^*Cl_3Ta(\eta^2\text{-}^{13}COSiMe_3)$ ($Cp^* = \eta^5\text{-}C_5Me_5$).[11c] The chemical shift of the carbonyl carbon in **9** (391.6 ppm) is at lower field than those of analogous zirconium acyls, by 70–90 ppm. This shift to lower field is also characteristic of a carbonyl group bound to silicon.[7,16] The ^{29}Si NMR spectrum (chloroform-d) contains a singlet at δ −2.66. Compound **9** has an electronic absorption in the visible region, 484 nm, attributable to a $\sigma \rightarrow \pi^*$ transition of the silaacyl ligand.[7,10c] Bis(silyl) ketones exhibit this transition in the visible region and are also pink.[17a] For comparison, the spectral properties of various acyl derivatives related to **9** are given in Table II.

This insertion reaction, forming a Si–C rather than a Si–O bond, is reversible (eq 5); on heating a toluene suspension of **9** to 80 °C for 2 h under a flow of nitrogen, decarbonylation to **1** occurs. Factors that should promote carbon monoxide insertion into the metal–silicon bond of **1** are (1) the increase in electron count at zirconium and (2) formation of a strong Zr–O bond. In keeping with this, we have observed CO insertion into the M–Si bonds of other electron-deficient early transition-metal silyls.[11c,e–g]

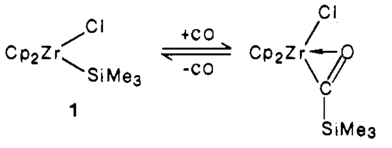

1 **9** (5)

Zirconium silyl **3**, in contrast to **1**, is not readily carbonylated. Attempted reaction of pentane or diethyl ether solutions of **3** with CO (100 psi) for 24 h resulted only in recovery of starting material. Monitoring the reaction by ^1H NMR (benzene-d_6, 30 psi CO) revealed the slow appearance (after several hours) of two peaks at 5.47 and 0.54 ppm with an intensity ratio of ca. 1:3, possibly due to $Cp_2Zr[\eta^2\text{-}COSi(SiMe_3)_3]Cl$ (**10**). After 7 days the [**10**]/[**3**] ratio had reached 0.4, but by then other products resulting from decomposition accounted for ca. 50% of the mixture. Although we cannot readily explain this decreased reactivity of **3** relative to **1**, we have observed that CO insertion is favorable in other group 4 metal–$Si(SiMe_3)_3$ derivatives.[11g] Among related alkyl derivatives, the rate of migratory CO insertion appears to increase as the alkyl group becomes more electron-releasing.[18] Due to delocalization of electron density by Si–Si bonds, the $Si(SiMe_3)_3$ group is expected to be less electron-donating than $SiMe_3$.[19]

Intramolecular competition experiments show that insertion of CO into $Zr\text{-}SiMe_3$ and Zr–Me bonds is favored over insertion into the $Zr\text{-}Si(SiMe_3)_3$ bond. Pentane solutions of **6** react rapidly with CO (100 psi) to give an orange solution from which silaacyl **11** can be crystallized in 70% yield (eq 6). This reaction is quantitative by ^1H NMR spectra (benzene-d_6, 20 psi CO). The presence of the $\eta^2\text{-}COSiMe_3$ ligand in **11** was established by comparison of spectral properties with **9** (Tables I and II) and by using ^{13}CO in the reaction. The ^1H NMR spectrum of ^{13}C-labeled **11** exhibits a doublet for the $\eta^2\text{-}^{13}COSiMe_3$ protons ($^3J_{CH}$ = 1.8 Hz). Insertion of CO into the Zr–C bond of the alkyl silyl **8** occurs to produce the acyl $Cp_2Zr(\eta^2\text{-}COMe)[Si(SiMe_3)_3]$ (**12**). In benzene-d_6 the latter reaction (20 psi CO) is quantitative by ^1H NMR.

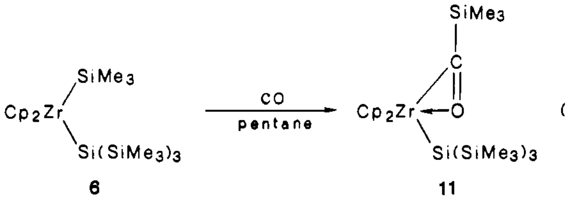

6 **11** (6)

The titanium silyl analogous to **1**, $Cp_2Ti(SiMe_3)Cl$[20] (**13**), reacts cleanly with CO by an apparent ligand-induced reductive elimination[21] (eq 7). This difference in behavior between Zr and Ti silyls **1** and **13** is attributed at least in part to the greater stability of lower valent compounds of Ti[22] and to a greater M–Cl bond strength for Zr.[23a] Reductive elimination involving an early transition-metal–chlorine bond would in general be unfavorable but in this case is facilitated by the high Si–Cl bond strength, 113 kcal mol^{-1}, for Me_3SiCl.[24] The mean bond dissociation energy for $TiCl_4$ is 103 kcal mol^{-1}.[23] Related reductive eliminations of Me_3SiCl have been observed in reactions of $Cp^*Cl_3TaSiMe_3$ with CO,[11c] alkynes,[11d] and PMe_3.[11d] In contrast, related titanium alkyls $Cp_2Ti(R)X$ are readily carbonylated to the acyls $Cp_2Ti(\eta^2\text{-}COR)X$,[25] which are also prepared by addition of alkyl halides to $Cp_2Ti(CO)_2$.[26] No reaction was observed between $Cp_2Ti(CO)_2$ and Me_3SiCl in benzene-d_6 after 3 days at room temperature and 7 h at 90 °C.

$$Cp_2Ti(SiMe_3)Cl \underset{\not\leftarrow}{\xrightarrow{CO}} Cp_2Ti(CO)_2 + Me_3SiCl \qquad (7)$$

These results show that various factors influence the course of reaction between a group 4 metal silyl and carbon monoxide. Additional reports from our laboratory will address further aspects of these trends.[11e–g]

Reactions of Zirconium–Silaacyl Complexes. Acylsilanes (R_3SiCOR') have a rich reaction chemistry that has been proven synthetically useful.[10] Much of this chemistry involves the 1,2-shift of silicon to oxygen, as in photochemically or thermally induced rearrangements to siloxy carbenes $R_3SiO\ddot{C}R'$.[27] Similar 1,2-silicon shifts may also result from nucleophilic attack at the carbonyl carbon.[10b] The formation of siloxide derivatives from silyl–carbonyl complexes (e.g., eq 1) might occur via such migrations in silaacyl intermediates.[28] To investigate this possibility and the reactivity of early transition-metal–η^2-silaacyl ligands in general, we have surveyed the reaction chemistry of **9** and **11**.

In related studies, it has been shown that the tantalum silaacyl $Cp^*Cl_3Ta(\eta^2\text{-}COSiMe_3)$ undergoes nucleophilic attack by carbon monoxide to give products derived from the transitory ketene $Cp^*Cl_3Ta[OC(CO)SiMe_3]$[11c] and by pyridines and phosphines to give tetrahedral adducts of the type $Cp^*Cl_3Ta[\eta^2\text{-}OC(SiMe_3)(L)]$ (A, L = pyridine, PMe_3, PEt_3, and $P(OMe)_3$),[11e] in which the $M\text{-}C_{acyl}$ bond is maintained. In contrast, **11** is unreactive toward pyridine (benzene-d_6, room temperature, 4 h). Addition of 1 equiv of pyridine to a dichloromethane-d_2 solution

---

(16) Dexheimer, E. M.; Buell, G. R.; Le Croix, C. *Spectrosc. Lett.* **1978**, *11*, 751.

(17) (a) Brook, A. G.; Jones, P. F.; Peddle, G. J. D. *Can. J. Chem.* **1968**, *46*, 2119. (b) Ricci, A.; Fiorenza, M.; Degl'Innocenti, A.; Seconi, G.; Dembech, P.; Witzgall, K.; Bestmann, H. J. *Angew. Chem., Int. Ed. Engl.* **1985**, *24*, 1068.

(18) (a) Bertelo, C. A.; Schwartz, J. *J. Am. Chem. Soc.* **1975**, *97*, 228. (b) Sonnenberger, D. C.; Mintz, E. A.; Marks, T. J. *J. Am. Chem. Soc.* **1984**, *106*, 3484. (c) Berke, H.; Hoffman, R. *J. Am. Chem. Soc.* **1978**, *100*, 7224.

(19) (a) Gilman, H.; Smith, C. L. *J. Organomet. Chem.* **1968**, *14*, 91. (b) Cook, M. A.; Eaborn, C.; Walton, D. R. M. *J. Organomet. Chem.* **1970**, *23*, 85.

(20) Rösch, L.; Altnau, G.; Erb, W.; Pickhardt, J.; Bruncks, N. *J. Organomet. Chem.* **1980**, *197*, 51.

(21) (a) McAlister, D. R.; Erwin, D. K.; Bercaw, J. E. *J. Am. Chem. Soc.* **1978**, *100*, 5966. (b) Yoshifuji, M.; Gell, K. I.; Schwartz, J. *Organomet. Chem.* **1978**, *153*, C15. (c) Gell, K. I.; Schwartz, J. *J. Chem. Soc., Chem. Commun.* **1979**, 244. (d) Gell, K. I.; Schwartz, J. *J. Am. Chem. Soc.* **1981**, *103*, 2687.

(22) Wailes, P. C.; Coutts, R. S. P.; Weigold, H. *Organometallic Chemistry of Titanium, Zirconium and Hafnium*; Academic Press: London, 1974.

(23) (a) Connor, J. A. In *Topics in Current Chemistry*; Springer-Verlag: New York, 1977; Vol. 71, pp 71–110. (b) Dias, A. R.; Salema, M. S.; Simões, J. A. M. *J. Organomet. Chem.* **1981**, *222*, 69.

(24) Walsh, R. *Acc. Chem. Res.* **1981**, *14*, 246.

(25) Fachinetti, G.; Floriani, C. *J. Organomet. Chem.* **1974**, *71*, C5.

(26) Fachinetti, G.; Floriani, C.; Stoeckli-Evans, H. *J. Chem. Soc., Dalton Trans.* **1977**, 2297.

(27) (a) Brook, A. G. *Acc. Chem. Res.* **1974**, *7*, 77. (b) Bassindale, A. R.; Brook, A. G.; Harris, J. *J. Organomet. Chem.* **1975**, *90*, C6. (c) Yates, P. *Pure Appl. Chem.* **1968**, *16*, 93. (d) Foster, A. M.; Agosta, W. C. *J. Am. Chem. Soc.* **1972**, *94*, 5777. (e) Bourque, R. A.; Davis, P. D.; Dalton, J. C. *J. Am. Chem. Soc.* **1981**, *103*, 697.

(28) Intermolecular processes involving nucleophilic attack of a carbonyl oxygen onto a coordinated silyl ligand are also possible, see: Nicholson, B. K.; Simpson, J. *J. Organomet. Chem.* **1978**, *155*, 237.

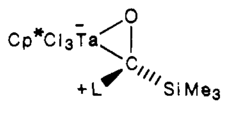

A

of **9** resulted only in a slight amount of decarbonylation to **1** after several hours.

Compound **9** does react with the isocyanide 2,6-$Me_2C_6H_3NC$ (eq 8); however, the adduct formed is a linear ketenimine **14** rather than a tetrahedral adduct such as A. Assignment of the structure of **14** is based on comparisons with spectral data for the known ketenimine $Cp_2{}^*Th[OC(CH_2CMe_3)(CN\text{-}2,6\text{-}Me_2C_6H_3)]Cl$, formed analogously from the acyl $Cp_2{}^*Th(\eta^2\text{-}COCH_2CMe_3)Cl$ and 2,6-$Me_2C_6H_3NC$.[29b] The ^{13}C NMR spectrum of **14** contains resonances due to C_α and C_β ($C_\beta{=}C_\alpha{=}N$) at δ 202.3 and 109.9, respectively. The corresponding ^{13}C NMR shifts for $Cp_2{}^*Th[OC(CH_2CMe_3)(CN\text{-}2,6\text{-}Me_2C_6H_3)]Cl$ appear at δ 216.8 and 110.3. Also in accord with the assigned ketenimine structure, the infrared spectrum of **14** contains a ν(CCN) absorption at 1977 cm^{-1}. Although **14** forms quantitatively in dichloromethane-d_2 (IR and NMR), attempts at isolation failed due to decomposition during workup (see Experimental Section).

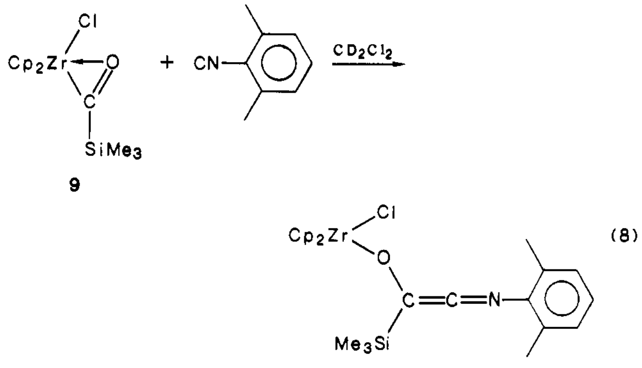

9

14

Reaction of **9** with $LiOCMe_3$ in diethyl ether (eq 9) proceeds with decarbonylation to give the silyl complex $Cp_2Zr(SiMe_3)(OCMe_3)$[11a] (88% yield). This process may reflect the ability of a lone pair on the butoxide ligand to compete favorably with the silaacyl oxygen for the same orbital on zirconium[15b] and implies that the η^2 geometry is important in stabilizing the silaacyl ligand. The nucleophilic reagents LiPh, $LiBH_4$, and $KOSiMe_3$ all react with **9** in diethyl ether to give off-white powders that exhibit very broad, featureless peaks in the Cp and $SiMe_3$ regions of their ^1H NMR spectra.

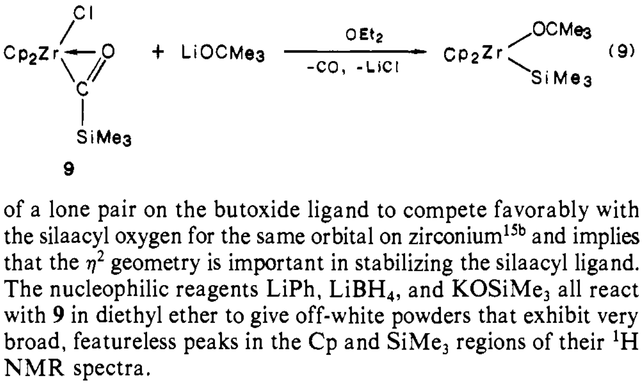

9

Reactions of **9** with electrophiles (E) were examined as possible routes to acylsilane derivatives ($ECOSiMe_3$). Interaction of **9** with an excess of $Me_3SiOSO_2CF_3$ in dichloromethane results in isolation of the light orange triflate $Cp_2Zr(\eta^2\text{-}COSiMe_3)(OSO_2CF_3)$ (**15**) in 62% yield (eq 10). Apparently, π-donation from the triflate ligand is not strong enough to induce decarbonylation in **15**. A similar chloride–triflate exchange occurs on treatment of **9** with $MeOSO_2CF_3$ in dichloromethane.

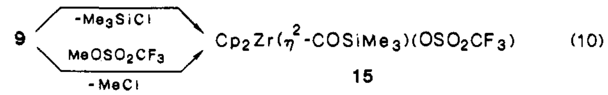

15

Acidification of zirconium acyls is a known route to aldehydes.[15e] We, therefore, attempted syntheses of the unknown formylsilane Me_3SiCHO by reactions of **9** and **11** with acids. Reaction of **9** with 1 equiv of HCl in dichloromethane-d_2 produced Cp_2ZrCl_2 quantitatively, along with a complex mixture of uncharacterized organosilicon products. Monitoring the reaction by variable temperature ^1H NMR (dichloromethane-d_2) revealed the appearance at −65 °C of a resonance at δ 11.77. This peak, possibly due to Me_3SiCHO, grew in intensity as the solution was warmed to −25 °C. Above this temperature, the product began to decompose and was not stable at room temperature.[30] Further spectroscopic evidence for the formylsilane was obtained from reaction of HCl with $Cp_2Zr(\eta^2\text{-}{}^{13}COSiMe_3)Cl$ at −65 °C, which gave a doublet at 11.77 (J_{CH} = 141 Hz). Corresponding to this coupling was a doublet in the ^{13}C NMR spectrum (−65 °C) at 248.9 ppm (J_{CH} = 141 Hz). The latter chemical shift is in the region expected for a $-COSiMe_3$ group.[16]

The analogous reaction of **11** with HCl gave a quantitative yield of $HSi(SiMe_3)_3$ and uncharacterized insoluble materials. Curiously, benzoic acid removes $-COSiMe_3$ instead of $-Si(SiMe_3)_3$ from **11** to give $Cp_2Zr[Si(SiMe_3)_3](\eta^2\text{-}O_2CPh)$ (**16**, eq 11) as the principle zirconium-containing product.

$$\underset{\mathbf{11}}{Cp_2Zr(\eta^2\text{-}COSiMe_3)Si(SiMe_3)_3} + HO_2CPh \rightarrow \underset{\mathbf{16}}{Cp_2Zr[Si(SiMe_3)_3](\eta^2\text{-}O_2CPh)} + \ldots \quad (11)$$

The formylsilane Me_3SiCHO was not detected in the reaction product mixture (by ^1H NMR). On the basis of the difference between $\nu_{asym}(CO_2)$ and $\nu_{sym}(CO_2)$ infrared stretching frequencies (98 cm^{-1}), it appears likely that the benzoate ligand in **16** is bidentate.[31]

Attempts at Other Insertion Reactions. The reactivity of a Zr–Si bond toward a nonpolar substrate was first observed in the reaction of **1** with hydrogen (100 psi, diethyl ether, room temperature) to give $[Cp_2ZrHCl]_n$ and $HSiMe_3$. This reaction occurs within minutes, as does the reaction between **6** and hydrogen (1 atm, benzene-d_6, room temperature) affording $HSiMe_3$ and $HSi(SiMe_3)_3$ quantitatively by ^1H NMR. Given the reactivity of Zr–Si bonds toward hydrogen and carbon monoxide, it was of interest to investigate the general propensity of zirconium silyls to add to unsaturated molecules.

Insertion of the isocyanide 2,6-$Me_2C_6H_3NC$ into the Zr–Si bonds of **1** and **3** occurs readily (eq 12). The yellow, crystalline products **17** and **18** exhibit spectroscopic features (Table I) that closely resemble those observed for the related η^2-iminoacyls $Cp_2Zr[\eta^2\text{-}C(NC_6H_4\text{-}p\text{-}Me)R]R'$ (R = alkyl; R′ = alkyl, Cl).[15j]

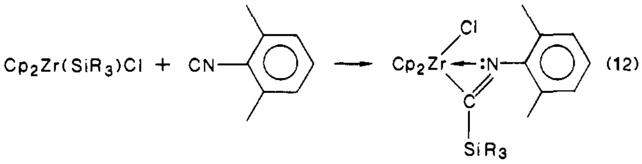

17, R = Me
18, R = $SiMe_3$

Unfortunately, we have been unable to observe reactions of **1** with ethylene (90 psi, diethyl ether, 2 days), phenylacetylene (excess, hexane, 1 day), benzonitrile (1 equiv, benzene-d_6, 1 day), carbon dioxide (100 psi, diethyl ether, 2 days), or carbon disulfide (excess, benzene-d_6, 1 day). Also, compound **3** does not react with phenylacetylene (excess, benzene-d_6, 90 °C, 1 day), 4-methoxybenzonitrile (1 equiv, benzene-d_6, 1 day), or phenyl isocyanate (1 equiv, benzene-d_6, 1 day). Our observations that Zr–Si bonds insert carbon monoxide and isonitriles but not many other un-

---

[29] (a) Fagan, P. J.; Manriquez, J. M.; Marks, T. J.; Day, V. W.; Vollmer, S. H.; Day, C. S. *J. Am. Chem. Soc.* **1980**, *102*, 5393. (b) Moloy, K. G.; Fagan, P. J.; Manriquez, J. M.; Marks, T. J. *J. Am. Chem. Soc.* **1986**, *108*, 56.

[30] Other attempts to prepare Me_3SiCHO: (a) Sommer, L. H.; Bailey, D. L.; Goldberg, G. M.; Buck, C. E.; Bye, T. S.; Evans, F. J.; Whitmore, F. C. *J. Am. Chem. Soc.* **1954**, *76*, 1613. (b) Speier, J. L., Jr. Ph.D. Thesis, University of Pittsburgh, 1947. (c) Sandman, D. J., personal communication.

[31] (a) Deacon, G. B.; Philips, R. J. *Coord. Chem. Rev.* **1980**, *33*, 227. (b) Hoffman, D. M.; Chester, N. D.; Fay, R. C. *Organometallics* **1983**, *2*, 48.

Table I. Spectroscopic Properties for New Compounds

compound	IR[a]		^1H NMR[b]		^{13}C NMR[c]	
$Cp_2Z[Si(SiMe_3)_3]Cl$ (**3**)			$SiMe_3$	0.40	$SiMe_3$	5.11
			C_5H_5	5.97	C_5H_5	111.2
$Cp_2Hf[Si(SiMe_3)_3]Cl$ (**4**)			$SiMe_3$	0.41	$SiMe_3$	5.35
			C_5H_5	5.89	C_5H_5	110.4
$Cp_2ClZr(\mu\text{-}O)ZrCp_2[Si(SiMe_3)_3]$ (**5**)			$Si(SiMe_3)_3$	0.49	$Si(SiMe_3)_3$	5.79
			C_5H_5	5.94	C_5H_5	109.7
			C_5H_5	6.08	C_5H_5	110.1
$Cp_2Zr[Si(SiMe_3)_3](SiMe_3)$ (**6**)			$SiMe_3$	−0.02	$SiMe_3$	1.15
			$Si(SiMe_3)_3$	0.28	$Si(SiMe_3)_3$	5.08
			C_5H_5	6.13	C_5H_5	108.3
$Cp_2Zr[Si(SiMe_3)_3]BH_4$ (**7**)	ν_{ZrBH_4}	2449, 2403, 2248, 2020, 1947, 1926, 1378, 1127	$SiMe_3$	0.39	$SiMe_3$	5.03
			C_5H_5	5.72	C_5H_5	106.9
$Cp_2Zr[Si(SiMe_3)_3]Me$ (**8**)			ZrMe	−0.36	$SiMe_3$	5.29
			$SiMe_3$	0.36	ZrMe	47.1
			C_5H_5	5.95	C_5H_5	109.6
$Cp_2Zr(\eta^2\text{-}COSiMe_3)Cl$ (**9**)[d]	ν_{CO}	1489	$SiMe_3$	0.47	$SiMe_3$	−2.90
			C_5H_5	5.78	C_5H_5	109.2
					ZrCOSi	391.6
$Cp_2Zr(\eta^2\text{-}COSiMe_3)[Si(SiMe_3)_3]$ (**11**)	ν_{CO}	1503	$COSiMe_3$	0.04	$COSi\mathit{Me}_3$	−3.55
			$Si(SiMe_3)_3$	0.59	$Si(SiMe_3)_3$	6.16
			C_5H_5	5.39	C_5H_5	103.8
					ZrCOSi	387.3
$Cp_2Zr(\eta^2\text{-}COMe)[Si(SiMe_3)_3]$ (**12**)	ν_{CO}	1505	$Si(SiMe_3)_3$	0.54	$Si(SiMe_3)_3$	5.96
			COMe	2.15	$CO\mathit{Me}$	33.2
			C_5H_5	5.39	C_5H_5	104.0
					ZrCO	312.3
$Cp_2Zr[OC(SiMe_3)(CN\text{-}2,6\text{-}Me_2C_6H_3)]Cl$ (**14**)[d]	ν_{CNN}	1977[e]	$SiMe_3$	0.17	$SiMe_3$	−1.85
			$\mathit{Me}_2C_6H_3$	2.36	$\mathit{Me}_2C_6H_3$	19.2
			C_5H_5	6.34	$\mathit{C}CN$	109.9
			C_6H_3	7.06 (m)	C_5H_5	114.5
					C_6H_3	125.6
						128.8
						130.6
						142.0
					$C\mathit{C}N$	202.3
$Cp_2Zr(\eta^2\text{-}COSiMe_3)(OSO_2CF_3)$ (**15**)[d]	ν_{CO}	1500	$COSiMe_3$	0.51	$SiMe_3$	−2.85
			C_5H_5	5.90	C_5H_5	110.0
					ZrCOSi	389.7
$Cp_2Zr[Si(SiMe_3)_3](\eta^2\text{-}O_2CPh)$ (**16**)	ν_{CO_2}	1593, 1495	$SiMe_3$	0.53	$SiMe_3$	5.80
			C_5H_5	5.94	C_5H_5	109.4
			Ph	7.05	Ph	128.5
				8.03		129.5
						131.4
						133.5
					ZrO_2C	182.3
$Cp_2Zr[\eta^2\text{-}C(N\text{-}2,6\text{-}Me_2C_6H_3)SiMe_3]Cl$ (**17**)	ν_{CN}	1558	$SiMe_3$	−0.09	$SiMe_3$	−1.80
			$\mathit{Me}_2C_6H_3$	1.93	$\mathit{Me}_2C_6H_3$	19.1
			C_5H_5	5.79	C_5H_5	109.8
			C_6H_3	6.82	C_6H_3	125.6
						128.7
						129.0
						148.0
					ZrCNSi	275.6
$Cp_2Zr[\eta^2\text{-}C(N\text{-}2,6\text{-}Me_2C_6H_3)Si(SiMe_3)_3]Cl$ (**18**)	ν_{CN}	1555	$SiMe_3$	0.18	$SiMe_3$	3.30
			$\mathit{Me}_2C_6H_3$	2.02	$\mathit{Me}_2C_6H_3$	20.7
			C_5H_5	5.89	C_5H_5	110.1
			C_6H_3	6.82	C_6H_3	126.0
						128.9
						129.7
						148.6
					ZrCNSi	267.6

[a] Nujol mull, except as noted. [b] Shifts in ppm, referenced to $SiMe_4$ (δ 0.00) at 300 MHz and 22 °C in benzene-d_6, except as noted. [c] Shifts are in ppm, referenced to $SiMe_4$ (δ 0.00) at 75.5 MHz and 22 °C in benzene-d_6, except as noted. [d] NMR spectra taken in dichloromethane-d_2. [e] IR spectrum taken in dichloromethane-d_2.

saturated substrates suggest that for zirconocene derivatives the reactivity of Zr–Si bonds parallels Zr–C bonds more closely than Zr–H bonds, which are known to add a wide variety of unsaturated substrates.

Description of the Structure of 9. The molecular structure of **9** is shown in Figure 1 with the atom labeling scheme. Crystal and data collection parameters are summarized in Table III. Tables IV and V list positional parameters and bond distances and angles, respectively. The structure consists of well-separated molecules with no abnormally short intermolecular contacts. Each molecule has approximate noncrystallographic mirror symmetry across the plane containing Zr, Cl, C11, and O. These four atoms lie in a plane to within ±0.005 Å, with the Si atom 0.04 Å out of this plane. The O–C11–Si–C13 torsion angle is 163.1°.

The structure is similar to that found in the acyl $Cp_2Zr(\eta^2\text{-}COMe)Me$.[15g] Distances and angles within the ZrOC triangle of **9** are identical with those found in $Cp_2Zr(\eta^2\text{-}COMe)[(OC)_3MoCp]$,[15a] exhibiting the same slight C–O bond elongation

Table II. Spectral Properties of Acyl Compounds

compound	ν_{CO},[a] cm^{-1}	λ_{max},[d] nm	^{13}C NMR,[f] δ_{CO}
PhCOPh[7]	1654	345 (130)	196.4[g]
$Ph_3SiCOPh$[7]	1614	424 (290)	230.7[h]
$Ph_3SiCOSiPh_3$[16a]	1558	554	
$Me_3SiCOSiMe_3$[17b]	1570		318.8
fac-$Re(CO)_3$(diphos)($COSiPh_3$)[7]	1490	557 (390)[e]	340.1[h]
$Cp_2Zr(\eta^2\text{-}COSiMe_3)Cl$ (**9**)	1489[b]	484 (106)[e]	391.6
$Cp_2Zr(\eta^2\text{-}COSiMe_3)(OSO_2CF_3)$ (**15**)	1500[b]		389.7
$Cp_2Zr(\eta^2\text{-}COSiMe_3)[Si(SiMe_3)_3]$ (**11**)	1503[b]	427 (232)[e]	387.3
$Cp^*Cl_3Ta(\eta^2\text{-}COSiMe_3)$[11c]	1462[b]		351
$Cp_2Zr(\eta^2\text{-}COCH_2CMe_3)Cl$[15j]	1550[b]		318.7[g]
$Cp_2Zr[\eta^2\text{-}CO(4\text{-}MeC_6H_4)]$-($4\text{-}MeC_6H_4$)[15h]	1505[c]		301[i]
$Cp^*_2Th(\eta^2\text{-}COCH_2CMe_3)Cl$[29]	1469	420 (140)[j]	360.2

[a] KBr pellet except as noted. [b] Nujol mull. [c] CH_2Cl_2 solution, −78 °C. [d] CCl_4 solution except as noted, molar absorptivity in parentheses. [e] CH_2Cl_2 solution. [f] C_6D_6 solution, except as noted. [g] $CDCl_3$ solution. [h] CD_2Cl_2 solution. [i] $CD_2Cl_2/CDCl_3$ solution, −75 °C. [j] Tetrahydrofuran solution.

Table III. Crystal and Data Collection Parameters for **9**

(A) Crystal Parameters at 25 °C[a,b]

a = 9.7608 (12) Å
b = 12.8694 (16) Å
c = 12.6837 (15) Å
β = 91.074 (10)°
V = 1593.0 (6) $Å^3$
size of cryst: 0.18 × 0.27 × 0.45 mm
space group: $P2_1/n$
formula = 358.07 amu
Z = 4
d = 1.49 g cm^{-3}
μ_{calcd} = 9.09 cm^{-1}

(B) Data Measurement Parameters

radiatn: Mo Kα (λ = 0.71073 Å)
monochrmtor: highly oriented graphite (2θ = 12.2°)
detctr: cryst scintlltn countr, with PHA
reflecns measd: $+h,+k,\pm l$
2θ range: 3° → 45°, scan type: θ–2θ
scan width: $\Delta\theta = 0.55 + 0.347 \tan(\theta)$
scan speed: 0.66 → 6.7 (θ, deg/min)
backgrnd: measd over 0.25($\Delta\theta$) added to each end of scan
aperture → cryst = 173 mm, vertcl aperture = 3.0 mm
horzntl aperture = 2.0 + 1.0 tan(θ) mm (variable)
no. of reflcns collctd: 2337
no. of unique reflcns: 2081
intensity standards: (553), (147), (38$\bar{2}$); measd every h of X-ray exposure time[c]
orienttn: 3 reflcns were checked after every 250 measrmnts

[a] Unit cell parameters and their esd's were derived by a least-squares fit to the setting angles of the unresolved Mo Kα components of 24 reflections with 2θ between 25° and 29°. [b] In this and all subsequent tables the esd's of all parameters are given in parentheses, right justified to the least significant digit(s) given. [c] Over the data collection period no decrease in intensity was observed. [d] Crystal orientation was redetermined if any of the reflections were offset from their predicted positions by more than 0.1°. Reorientation was needed once during data collection.

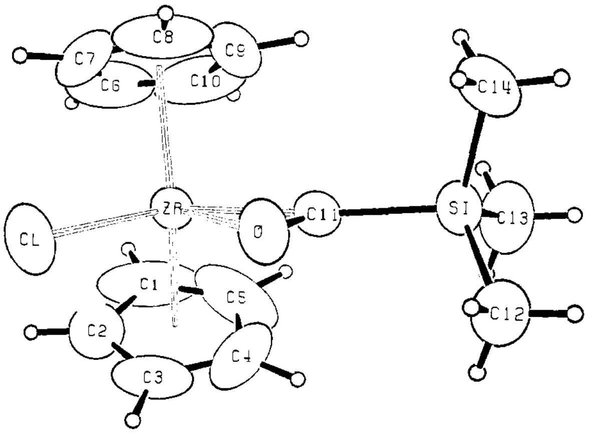

Figure 1. Ortep view of **9** with atom-labeling scheme.

Table IV. Positional Parameters and Their esd's for **9**[a]

atom	x	y	z	B ($Å^2$)
Zr	0.19664 (3)	0.15052 (2)	0.23025 (2)	2.698 (6)
Cl	0.03874 (9)	−0.00356 (7)	0.19996 (8)	5.24 (2)
Si	0.61098 (9)	0.11677 (7)	0.22323 (7)	3.67 (2)
O	0.3549 (2)	0.0270 (2)	0.2031 (2)	4.05 (5)
C1	0.1133 (3)	0.3101 (2)	0.1399 (2)	8.7 (1)
C2	0.0526 (2)	0.2311 (2)	0.0882 (2)	6.5 (1)
C3	0.1497 (3)	0.1785 (2)	0.0372 (2)	6.0 (1)
C4	0.2710 (2)	0.2243 (2)	0.0583 (2)	7.2 (1)
C5	0.2487 (2)	0.3052 (2)	0.1228 (2)	9.1 (1)
C6	0.0863 (2)	0.2405 (2)	0.3785 (3)	10.6 (1)
C7	0.0798 (2)	0.1407 (2)	0.4033 (3)	10.3 (1)
C8	0.2064 (3)	0.1069 (2)	0.4217 (3)	7.9 (1)
C9	0.2913 (2)	0.1869 (2)	0.4097 (3)	7.8 (1)
C10	0.2165 (3)	0.2693 (2)	0.3822 (3)	8.1 (1)
C11	0.4136 (3)	0.1111 (2)	0.2209 (2)	3.21 (6)
C12	0.6672 (4)	0.0359 (3)	0.1124 (3)	5.8 (1)
C13	0.6653 (4)	0.2532 (3)	0.2110 (4)	6.2 (1)
C14	0.6645 (4)	0.0595 (4)	0.3520 (3)	6.1 (1)

[a] Anisotropically refined atoms are given in the form of the isotropic equivalent thermal parameter defined as $(^4/_3)[a^2B(1,1) + b^2B(2,2) + c^2B(3,3) + ab(\cos\gamma)B(1,2) + ac(\cos\beta)B(1,3) + bc(\cos\alpha)B(2,3)]$.

Table V. Bond Distances (Å) and Angles (deg) for **9**[a]

Distances[b]			
Zr–Cl	2.536 (1)	C11–O	1.244 (3)
Zr–O	2.248 (1)	C11–Si	1.927 (2)
Zr–C11	2.183 (2)	Si–C12	1.841 (3)
Zr–CP1	2.212	Si–C13	1.842 (3)
Zr–CP2	2.210	Si–C24	1.858 (3)
Zr–C1	2.482 (3)	C1–C2	1.342 (2)
Zr–C2	2.491 (2)	C2–C3	1.341 (2)
Zr–C3	2.508 (3)	C3–C4	1.345 (2)
Zr–C4	2.499 (3)	C4–C5	1.344 (2)
Zr–C5	2.470 (3)	C5–C1	1.345 (2)
Zr–C6	2.472 (3)	C6–C7	1.324 (2)
Zr–C7	2.495 (3)	C7–C8	1.326 (2)
Zr–C8	2.492 (3)	C8–C9	1.332 (2)
Zr–C9	2.485 (3)	C9–C10	1.330 (2)
Zr–C10	2.465 (3)	C10–C6	1.324 (2)

Angles[c]			
Cl–Zr–O	80.86 (4)	Zr–O–C11	70.88 (12)
O–Zr–C11	32.56 (7)	Zr–C11–O	76.55 (13)
Cl–Zr–C11	113.42 (6)	Zr–C11–Si	163.87 (13)
CP1–Zr–Cl	105.04	O–C11–Si	119.56 (16)
CP1–Zr–O	111.39	C11–Si–C12	106.20 (11)
CP2–Zr–C11	101.69	C11–Si–C13	108.90 (12)
CP2–Zr–Cl	104.79	C11–Si–C14	105.23 (12)
CP2–Zr–O	112.42	C12–Si–C13	112.60 (15)
CP2–Zr–C11	102.14	C12–Si–C14	111.37 (16)
CP2–Zr–CP1	129.88	C13–Si–C14	112.06 (15)

[a] CP1 and CP2 are the centroids of the cyclopentadienyl rings. [b] Bond distances in the C_5H_5 rings were constrained to be equal ±0.002 Å. [c] Bond angles in the C_5H_5 rings were constrained to be 108.0 ± 0.1°.

and Zr–O bond contraction relative to $Cp_2Zr(\eta^2\text{-}COMe)Me$. The Si–C(acyl) bond length of 1.927 (2) Å is slightly shorter than the corresponding distance in *fac*-$Re(CO)_3$(dppe)($COSiPh_3$) (1.969 (10) Å), but it is considerably longer than the average of the remaining Si–C(Me) bond lengths, 1.847 (7) Å, a feature also observed in *fac*-$Re(CO)_3$(dppe)($COSiPh_3$)[7] and in $Ph_3SiCOMe$.[32]

Experimental Section

All manipulations were conducted under an inert atmosphere of nitrogen or argon. All solvents were distilled from sodium benzophenone ketyl before use, except dichloromethane, which was distilled from calcium hydride. The compounds $Cp_2Zr(SiMe_3)Cl$,[11a] $(THF)_3LiSi(SiMe_3)_3$,[13] $Cp_2Ti(SiMe_3)Cl$,[20] and $(Cp_2ZrCl)_2(\mu\text{-}O)$[33] were prepared according to the literature procedures. The compounds $Me_3SiOSO_2CF_3$

---

(32) Chieh, P. C.; Trotter, J. *J. Chem. Soc. A* **1969**, 1778.

(33) Reid, A. F.; Shannon, J. S.; Swan, J. M.; Wailes, P. C. *Aust. J. Chem.* **1965**, *18*, 173.

(Petrarch), $MeOSO_2CF_3$ (Aldrich), and $2,6\text{-}Me_2C_6H_3NC$ (Fluka) were used as received. Elemental analyses were performed by Galbraith or Schwartzkopf microanalytical laboratories. Although **8**, **11**, **12**, and **18** gave carbon analyses that were variable and somewhat low, the spectroscopic data show that these compounds are pure and correctly formulated. We have experienced this problem with other compounds containing the $-Si(SiMe_3)_3$ group and suggest that it is due to formation of silicon carbide, which does not burn completely, during the combustion analysis.

Infrared spectra were recorded on a Perkin-Elmer 1330 infrared spectrometer. Electronic spectra were recorded on an IBM 9420 UV-vis spectrophotometer. ^1H NMR spectra were recorded at 360 MHz with a spectrometer fabricated locally by Dr. John Wright, at 90 MHz with a Varian EM-390, or at 300 MHz with a GE QE-300 instrument. $^{13}C\{^1H\}$ NMR spectra were recorded at 50.3 MHz with a Nicolet WB-200 spectrometer or at 75.5 MHz on the GE QE-300. $^{29}Si\{^1H\}$ spectra were recorded at 59.6 MHz on the GE QE-300. An INEPT sequence was employed to enhance signals in the ^{29}Si spectra.[34] GC analyses were conducted on a Varian 3400 instrument coupled to a Varian 4290 integrator, by using a 3 m × $^1/_8$ in. stainless steel column with 25% 1,2,3-tris(2-cyanoethoxy)propane as stationary phase.

$Cp_2Zr[Si(SiMe_3)_3]Cl$ (3). Diethyl ether (60 mL) was added to a flask containing Cp_2ZrCl_2 (1.00 g, 3.42 mmol) and $(THF)_3LiSi(SiMe_3)_3$ (1.61 g, 3.42 mmol). After stirring the red-orange solution for 2 days, the volatiles were removed under vacuum. The resulting orange residue was extracted with pentane (2 × 25 mL), and the combined extracts were concentrated and cooled (−15 °C) to afford red-orange crystals of **3** (mp 214–215 °C, dec) in 70% yield (1.21 g): IR (Nujol, CsI, cm^{-1}) 1235 m, 1012 m, 825 s, 795 s, 672 m, 619 m, 345 w. Anal. Calcd for $C_{19}H_{37}ClSi_4Zr$: C, 45.2; H, 7.39; Cl, 7.03; Si, 22.3. Found: C, 45.0; H, 7.40; Cl, 6.86; Si, 22.1.

$Cp_2Hf[Si(SiMe_3)_3]Cl$ (4). The procedure for compound **3** was followed by using Cp_2HfCl_2 (0.40 g, 1.05 mmol) and $(THF)_3LiSi(SiMe_3)_3$ (0.50 g, 1.06 mmol). Yellow needles of **4** (dec > 150 °C) were isolated in 68% yield (0.42 g): IR (Nujol, CsI, cm^{-1}) 1442 w, 1237 s, 1016 m, 830 vs, 803 s sh, 744 w, 730 w, 672 m, 619 m, 312 m br. Anal. Calcd for $C_{19}H_{37}ClHfSi_4$: C, 38.6; H, 6.30; Cl, 5.99; Si, 18.9. Found: C, 38.9; H, 6.46; Cl, 6.24; Si, 19.1.

$Cp_2(Cl)Zr(\mu\text{-}O)ZrCp_2[Si(SiMe_3)_3]$ (5). Diethyl ether was added to a flask containing $(Cp_2ZrCl)_2(\mu\text{-}O)$ (0.161 g, 0.21 mmol) and $(THF)_3LiSi(SiMe_3)_3$ (0.135 g, 0.21 mmol) at room temperature. The resulting yellow solution was stirred for 16 h, the diethyl ether was removed under reduced pressure, and the resulting yellow solid was extracted with pentane (3 × 15 mL). Concentration and cooling (−40 °C) of the combined pentane extracts afforded a yellow solid, contaminated slightly with impurities (by ^1H NMR) in 45% yield (0.070 g). Further purification was achieved by recrystallization from pentane (mp 215–220 °C): IR (Nujol, CsI, cm^{-1}) 1260 w, 1240 w, 1015 w, 830 m, 800 m, 705 m, 680 w sh, 620 w, 339 w. Anal. Calcd for $C_{29}H_{47}ClOSi_4Zr_2$: C, 47.0; H, 6.38. Found: C, 47.2; H, 6.06.

$Cp_2Zr[Si(SiMe_3)_3]SiMe_3$ (6). Compound **1** (0.40 g, 1.21 mmol) and $(THF)_3LiSi(SiMe_3)_3$ (0.57 g, 1.21 mmol) were placed in a flask and cooled to −78 °C. Cold (−78 °C) diethyl ether (40 mL) was added, and the mixture allowed to warm to room temperature. After 3 h of additional stirring the volatiles were removed by vacuum transfer, and the resulting residue was extracted with pentane (45 mL). Concentration and cooling (−40 °C) of the pentane solution resulted in crystallization of very dark red prisms (mp 117–121 °C) in 70% yield (0.46 g): IR (Nujol, CsI, cm^{-1}) 1239 s, 1017 m, 830 vs, 796 s sh, 746 w, 724 m, 675 m, 662 w sh, 620 m, 412 w, 385 w; $^{29}Si\{^1H\}$ NMR (benzene-d_6, 59.6 MHz) δ −80.33 ($Zr\mathit{Si}(SiMe_3)_3$), −5.89 ($ZrSi(\mathit{Si}Me_3)_3$), 22.30 ($Zr\mathit{Si}Me_3$). Anal. Calcd for $C_{22}H_{46}Si_5Zr$: C, 48.7; H, 8.55. Found: C, 48.3; H, 8.53.

$Cp_2Zr[Si(SiMe_3)_3]BH_4$ (7). A flask was charged with **3** (0.50 g, 0.99 mmol) and $LiBH_4$ (0.0022 g, 1.01 mmol) and then cooled to −78 °C. Cold (−78 °C) diethyl ether (50 mL) was added, and the mixture was stirred for 24 h. Removal of solvent under vacuum, extraction of the residue with pentane (2 × 30 mL), and concentration and cooling of the combined pentane extracts afforded yellow crystals (mp 154–155 °C) in 68% yield (0.33 g): IR (Nujol, CsI, cm^{-1}) $\nu(ZrBH_4)$ 2449 m, 2443 m, 2248 w, 2020 w, 1947 m, 1926 m, 1378 m (assigned in Fluorolube mull spectrum), 1127 m; other peaks 1257 w, 1242 m, 1015 m, 830 vs, 800 s sh, 679 m, 622 m. Anal. Calcd for $C_{19}H_{41}BSi_4Zr$: C, 47.2; H, 8.54; B, 2.23. Found: C, 47.6; H, 9.05; B, 2.07.

$Cp_2Zr[Si(SiMe_3)_3]Me$ (8). A diethyl ether solution (25 mL) of **3** (0.50 g, 0.99 mmol) was cooled to −78 °C, and MeMgBr (0.35 mL of a 2.0 M diethyl ether solution, 0.99 mmol) was added. After having been stirred for 10 min at −78 °C, the solution was allowed to warm to room temperature. The volatiles were removed by vacuum transfer, and the resulting residue was extracted with pentane (40 mL). Concentration and cooling (−40 °C) the pentane solution gave the microcrystalline yellow-orange product (mp 173–175 °C) in 71% yield (0.34 g): IR (Nujol, CsI, cm^{-1}) 1251 w sh, 1236 m, 1014 m, 860 w sh, 830 s, 797 s, 745 w, 731 w, 676 m, 621 m, 420 vw, 342 vw. Anal. Calcd for $C_{20}H_{40}Si_4Zr$: C, 49.6; H, 8.33. Found: C, 48.4; H, 7.94.

$Cp_2Zr(\eta^2\text{-}COSiMe_3)Cl$ (9). Compound **1** (0.70 g, 2.12 mmol) was dissolved in diethyl ether (20 mL), and the solution was transferred to a pressure bottle. Pressurizing the solution with 100 psi of CO caused precipitation of 0.65 g of **9** as a pink powder. This powder, after washing with pentane or diethyl ether, is pure enough for most purposes. It was crystallized by diffusion of diethyl ether into a concentrated dichloromethane solution (mp 130–133 °C): IR (Nujol, CsI, cm^{-1}) 1489 m, 1252 m, 1012 m, 877 m sh, 842 vs, 802 vs, 753 m, 620 m, 339 m, 267 w, 247 m; $^{29}Si\{^1H\}$ NMR (chloroform-d, 59.6 MHz) δ −2.66. Anal. Calcd for $C_{14}H_{19}ClOSiZr$: C, 47.0; H, 5.35; Cl, 9.90. Found: C, 46.7; H, 5.39; Cl, 10.2.

$Cp_2Zr(\eta^2\text{-}COSiMe_3)[Si(SiMe_3)_3]$ (11). A solution of **6** (0.33 g, 0.61 mmol) in pentane (50 mL) was pressurized with CO (100 psi), resulting in a rapid color change from dark red to light orange. After 1 h, the CO pressure was released, and the solution was filtered, concentrated to ca. 5 mL, and cooled (−40 °C). The orange crystals (mp 140–142 °C) were isolated in 75% yield (0.26 g): IR (Nujol, CsI, cm^{-1}) 1503 m, 1250 m, 1238 m, 1013 m, 830 vs, 793 s, 747 m, 671 m, 620 m, 410 m; $^{29}Si\{^1H\}$ NMR (benzene-d_6, 59.6 MHz) δ −122.54 ($Zr\mathit{Si}(SiMe_3)_3$), −4.45 ($ZrCO\mathit{Si}Me_3$), −4.31 ($ZrSi(\mathit{Si}Me_3)_3$). Anal. Calcd for $C_{23}H_{46}OSi_5Zr$: C, 48.4; H, 8.13. Found: C, 47.2; H, 7.74.

$Cp_2Zr(\eta^2\text{-}COMe)[Si(SiMe_3)_3]$ (12). A pressure bottle was charged with **8** (0.255 g, 0.50 mmol) and pentane (25 mL). Addition of carbon monoxide (60 psi) was rapidly followed by precipitation of **12**. Recrystallization from pentane/tetrahydrofuran gave yellow crystals (mp 142–143 °C) in 73% yield (0.197 g): IR (Nujol, CsI, cm^{-1}) 1505 w, 1232 m, 1135 m, 1012 m, 860 m sh, 830 s, 670 m, 619 m. Anal. Calcd for $C_{21}H_{40}OSi_4Zr$: C, 49.2; H, 7.87. Found: C, 48.3; H, 8.10.

Reaction of 13 with Carbon Monoxide. A solution of $Cp_2Ti(SiMe_3)Cl$ (**13**) (0.40 g, 1.77 mmol) in diethyl ether (30 mL) was pressurized with CO (100 psi) and stirred. After 2 days the pressure was released; and the volatiles were removed by vacuum transfer. The residue was shown to be reasonably pure $Cp_2Ti(CO)_2$ by comparing spectral properties (^1H NMR and IR) with an authentic sample. The Me_3SiCl was identified among the volatiles by gas chromatography. When followed by ^1H NMR (benzene-d_6, ca. 2 atm CO, sealed NMR tube) the reaction was observed to go quantitatively to completion.

Reaction of 9 with $LiOCMe_3$. Diethyl ether (20 mL) was added to a mixture of **9** (0.30 g, 0.84 mmol) and $LiOCMe_3$ (0.067 g, 0.84 mmol). Stirring for 15 h resulted in a yellow solution and a white precipitate. Removal of volatiles, extraction with pentane (50 mL), and concentration and cooling of the pentane extract gave yellow crystals of $Cp_2Zr(SiMe_3)(OCMe_3)$[11a] in 88% yield.

$Cp_2Zr[OC(SiMe_3)(CN\text{-}2,6\text{-}Me_2C_6H_3)]Cl$ (14). Dichloromethane-d_2 (0.4 mL) was added to a 5-mm NMR tube containing **9** (0.020 g, 0.056 mmol) and $2,6\text{-}Me_2C_6H_3NC$ (0.008 g, 0.061 mmol). Within 5 min the pink solution turned yellow affording the product quantitatively by ^1H NMR and solution IR. This product is thermally stable in solution for 48 h at 90 °C: IR (dichloromethane-d_2, solution cell) 2950 m, 1977 s, 1496 w, 1461 m, 1435 m, 1311 m, 1242 s, 1101 s, 1071 m.

Preparative scale reactions were carried out in dichloromethane at −78 °C or at room temperature. The product, isolated as a yellow solid by either removal of solvent or by crystallization from diethyl ether, decomposes in the solid state to a red oil. By ^1H NMR this red oil consists of a complex mixture of decomposition products. Attempts to purify the red oil have been unsuccessful.

$Cp_2Zr(\eta^2\text{-}COSiMe_3)OSO_2CF_3$ (15). A solution of $Me_3SiOSO_2CF_3$ (0.37 g, 1.66 mmol) in dichloromethane (20 mL) was added to a dichloromethane (15 mL) solution of **9** (0.30 g, 0.84 mmol). After having been stirred for 10 h, the solution was evaporated to an orange residue and redissolved in dichloromethane (15 mL). Concentration and cooling (−78 °C) yielded light orange microcrystals in 61% yield (0.24 g): IR (Nujol, CsI, cm^{-1}) 1500 m, 1328 s, 1249 m, 1239 m, 1210 s, 1179 m, 1154 w sh, 1030 s, 877 m sh, 852 s sh, 805 s, 756 m, 745 m, 630 s, 510 m, 420 m, 349 m. Anal. Calcd for $C_{15}H_{19}F_3OSSiZr$: C, 38.2; H, 4.06; S, 6.80. Found: C, 38.2; H, 3.98; S, 7.22.

Reaction of 9 with $MeOSO_2CF_3$. An NMR tube was charged with compound **9** (0.030 g, 0.084 mmol) and dichloromethane-d_2 (0.35 mL). To the resulting pink solution was added $MeOSO_2CF_3$ (0.014 g, 0.084 mmol). Within 2 h the solution had turned orange. The ^1H NMR spectrum showed quantitative conversion to **15** and MeCl. The MeCl was further identified by ^{13}C NMR and GC analysis.

---

(34) Blinka, T. A.; Helmer, B. J.; West, R. *Adv. Organomet. Chem.* **1984**, *23*, 193.

$Cp_2Zr[Si(SiMe_3)_3](\eta^2\text{-}O_2CPh)$ (16). Benzene (40 mL) was added to a flask containing **11** (0.150 g, 0.23 mmol) and benzoic acid (0.031 g, 0.28 mmol). The initial orange solution turned yellow over 5 h, after which the volatiles were removed, and the resulting yellow solid was extracted with pentane (50 mL). Concentration and cooling (−40 °C) of the pentane solution afforded yellow crystals (mp 192–196 °C) in 44% yield (0.066 g): IR (Nujol, CsI, cm^{-1}) 1593 m, 1495 s, 1230 s, 1170 w, 1061 w, 1016 s, 860 s sh, 825 s, 792 s, 718 s, 689 m, 670 m, 619 s, 451 m, 341 w. Anal. Calcd for $C_{26}H_{42}O_2Si_4Zr$: C, 52.9; H, 7.29. Found: C, 53.4; H, 7.34. When monitored by ^{1}H NMR, the reaction was seen to proceed to **16** and other silicon-containing products that could not be identified.

$Cp_2Zr[\eta^2\text{-}C(N\text{-}2,6\text{-}Me_2C_6H_3)SiMe_3]Cl$ (17). To a flask containing **1** (0.25 g, 0.76 mmol) and $2,6\text{-}Me_2C_6H_3NC$ (0.10 g, 0.76 mmol) was added benzene (50 mL) at room temperature. After stirring the yellow solution for 1 h the solvent was removed, and the resulting yellow solid was extracted into pentane (2 × 40 mL). Concentration and cooling (−40 °C) of the combined pentane extracts afforded yellow crystals (mp 211–213 °C) in 68% yield (0.24 g): IR (Nujol, CsI, cm^{-1}) 1558 m, 1240 m, 1157 m, 1085 w, 1010 s, 870 m, 832 s, 780 s, 750 w, 659 w, 311 m. Anal. Calcd for $C_{22}H_{28}ClNSiZr$: C, 57.3; H, 6.11. Found: C, 56.7; H, 6.20.

$Cp_2Zr[\eta^2\text{-}C(N\text{-}2,6\text{-}Me_2C_6H_3)Si(SiMe_3)_3]Cl$ (18). Diethyl ether (80 mL) was added to a flask containing **3** (0.36 g, 0.71 mmol) and $2,6\text{-}Me_2C_6H_3NC$ (0.93 g, 0.71 mmol) at room temperature. Stirring for 5 h produced a clear yellow solution that on concentration and cooling (−40 °C) afforded yellow crystals (mp 223–225 °C, dec) in 75% yield (0.34 g): IR (Nujol, CsI, cm^{-1}) 1555 w, 1240 m, 1085 w, 1015 m, 825 br s, 789 s, 764 m, 680 m, 619 w, 350 w. Anal. Calcd for $C_{28}H_{46}ClNSiZr$: C, 52.9; H, 7.28. Found: C, 49.6; H, 6.94.

Reaction of 1 with Hydrogen. Compound **1** (0.30 g, 0.91 mmol) in diethyl ether was reacted with hydrogen gas (100 psi) for 18 h. This resulted in precipitation of an off-white solid that was shown to be $[Cp_2ZrHCl]_n$ by comparison of its spectral properties to an authentic sample and by its reaction with acetone to give $Cp_2Zr(OCHMe_2)Cl$.[35] Trimethylsilane was identified as a product by GC mass spectroscopy and by monitoring the reaction by ^{1}H NMR (benzene-d_6 solution).

Single-Crystal X-ray Diffraction Study of 9. Crystals were obtained by slow diffusion of diethyl ether into a concentrated dichloromethane solution of **9**. The crystals were mounted in thin-walled glass capillaries in an inert atmosphere glovebox, and the capillaries were flame sealed. Preliminary precession photographs indicated monoclinic Laue symmetry and yielded preliminary cell dimensions. The crystal used for data collection was then transferred to an Enraf-Nonius CAD-4 diffractometer[36] and centered in the beam. Automatic peak search and indexing procedures yielded the monoclinic reduced primitive cell. Systematic absences were consistent only with space group $P2_1/n$. The final cell parameters and specific data collection parameters are given in Table III.

The 2337 raw intensity data were converted to structure factor amplitudes and their esds by correction for scan speed, background, and Lorentz and polarization effects.[37] No correction for crystal decomposition was necessary. Inspection of the azimuthal scan data showed a variation $I_{min}/I_{max} = 0.89$ for the average curve. An empirical correction for absorption, based on the azimuthal scan data, was applied to the intensities, as the critical faces of the crystal were not well-defined. Removal of systematically absent and redundant data left 2081 unique data.

The structure was solved by Patterson methods and refined via standard least-squares and Fourier techniques. In a difference Fourier map calculated following refinement of all non-hydrogen atoms with anisotropic thermal parameters, peaks corresponding to the expected positions of most of the hydrogen atoms were found. Hydrogens were included in the structure factor calculations in their expected positions based on idealized bonding geometry but were not refined in least squares. They were assigned isotropic thermal parameters 1–2 Å^2 larger than the equivalent B_{iso} of the atom to which they were bonded. The carbon atoms of the cyclopentadiene rings showed large thermal motion, and the C–C distances refined poorly, so constraints were introduced into least squares such that within each Cp ring the distances would be equal and the angles would be the ideal 108.0°. A secondary extinction parameter[38] was refined in the final cycles of least squares. The final residuals[39] for 164 variables refined against the 1836 data for which $F^2 < 3\sigma(F^2)$ and 20 constraints were $R = 2.41\%$, $wR = 3.69\%$, and GOF = 1.963. The R value for all 2081 data was 3.10%.

The quantity minimized by the least-squares program was $\sum w(|F_o| - |F_c|)^2$, where w is the weight of a given observation. The p factor, used to reduce the weight of intense reflections, was set to 0.03 throughout the refinement. The analytical forms of the scattering factor tables for the neutral atoms were used,[40] and all non-hydrogen scattering factors were corrected for both the real and imaginary components of anomalous dispersion.[41] Inspection of the residuals ordered in ranges of $(\sin\theta)/\lambda, |F_o|$ and parity and value of the individual indexes showed no unusual features or trends. The largest peak in the final difference Fourier map had an electron density of 0.30 e$^-$/Å^3 and was located near C6.

Acknowledgment is made to the donors of the Petroleum Research Fund, administered by the American Chemical Society, to Research Corporation, and to the Air Force Office of Scientific Research (Grant No. AFOSR-85-0228) for support of this work. We thank Dr. D. J. Sandman for information regarding attempted syntheses of Me_3SiCHO.

Supplementary Material Available: A listing of general temperature factor expressions for **9** (1 page); a listing of observed and calculated structure factors for **9** (12 pages). Ordering information is given on any current masthead page.

---

(35) Gell, K. I.; Schwartz, J. *J. Am. Chem. Soc.* **1978**, *100*, 3246.

(36) The crystal structure was determined by Dr. F. J. Hollander, staff crystallographer at the U.C. Berkeley X-ray Crystallographic Facility (CHEXRAY).

(37) The data reduction formulas are $F_o^2 = (w/\text{Lp})(\text{C-2B})$, $\sigma_0(F_o^2) = (w/\text{Lp})(\text{C} + 4\text{B})^{1/2})$, $F_o = (F_o^2)^{1/2}$, and $\sigma_0(F) = \sigma_0(F_o^2)/2F_o$.

(38) Zachariesen, W. H. *Acta Crystallogr.* **1963**, *16*, 1139.

(39) $R = \sum||F_o| - |F_c||/\sum|F_o|$, $wR = \{\sum w|F_o| - |F_c|)^2/wF_o^2\}^{1/2}$, and GOF $= \{\sum w(|F_o| - |F_c|)^2/(n_0 - n_v)\}^{1/2}$.

(40) Cromer, D. T.; Waber, J. T. *International Tables for X-ray Crystallography*; The Kynoch Press: Birmingham, England, 1984; Vol. IV, Table 2.2B.

(41) Cromer, D. T., ref 35, Table 2.3.1.